



J. Serb. Chem. Soc. 82 (2) 203–213 (2017)
JSCS–4959

A new approach to synthesis and growth of nanocrystalline AlOOH with high pore volume

FARHAD SALIMI^{1*}, MOZAFFAR ABDOLLAHIFAR^{1,2**}, POURIA JAFARI¹
and MASOUD HIDARYAN¹

¹Department of Chemical Engineering, College of Science, Kermanshah Branch, Islamic Azad University, Kermanshah 67131, Iran and ²Department of Chemical Engineering, National Taiwan University, Taipei, 106, Taiwan

(Received 13 July, revised 9 November, accepted 14 November 2016)

Abstract: In this study, AlOOH nanostructures were successfully synthesized using the solvothermal method at 180 °C. The effects of the pH of the solution (3, 4.5, 6.5, 10 and 12.5) on the synthesized samples were investigated systematically in detail, when ethanol and NaOH were the solvent and pH-adjusting agent, respectively. Fourier transform infrared spectroscopy, X-ray powder diffraction and field emission scanning electron microscopy were used to characterize the synthesized samples. The specific surface area, pore size distribution and pore structure of different AlOOH structures at various pH levels were also discussed in terms of the N₂ adsorption/desorption test. According to the experimental results, the FESEM micrographs showed that the products were nanostructures, and the AlOOH nanoparticles larger on increasing the pH from 4.5 to 12.5. The structure characterization revealed that the resulting AlOOH nanostructures were pure and had a well-defined crystalline structure with a crystal size of 9.3–20.5 nm. Furthermore, the boehmite obtained at pH 12.5 exhibited a large surface area of 131 m² g⁻¹ and a high total pore volume of 1.24 cm³ g⁻¹.

Keywords: boehmite; pH; pore volume; nanostructures.

INTRODUCTION

Boehmite (AlOOH) and Al₂O₃ have attracted considerable research interest as they are widely used in the assembly of catalysts and catalyst supports,^{1–9} filters,¹⁰ abrasives,¹¹ membranes,^{12,13} adsorbents,¹⁴ various ceramics,^{15,16} optical devices¹⁷ and biomedical materials.¹⁸ Boehmite is an aluminium oxy-hydroxide which can be a frequently used precursor for the fabrication of Al₂O₃ materials.^{19,20} AlOOH, especially in a nanoscale size, is used as an additive in poly-

*** Corresponding authors. E-mail: (*)fasa348@yahoo.com; (**)abdollahifar@gmail.com
doi: 10.2298/JSC160713006S

mer materials,²¹ due to its low price, excellent mechanical properties, good chemical stability, and high surface area and large pore volume.

To date, boehmite has been successfully synthesized with different structures. Many researchers reported various morphologies of AlOOH, such as nanotubes,²² nanofibers,²³ nanowires,²⁴ sphere-like superstructures²⁵ and flower-like nanostructures with a high adsorption capacity.²⁶ The flower-like boehmite and alumina structures were synthesized by Abdollahifar *et al.*²⁰ and Zhang *et al.*²⁷ using hydrothermal and solvothermal methods, respectively. Abdollahifar¹⁷ controllably synthesized AlOOH and Al₂O₃ nanorods *via* the hydrothermal route. Using boehmite as a catalyst support, Baneshi *et al.*² synthesized CuO/ZrO₂/Al₂O₃ and CuO/CeO₂/Al₂O₃ nanocatalysts, which showed higher catalytic activity. Other hierarchical boehmite nanostructures were also synthesized using different methods.^{28–35}

The synthesis method has an important effect on the properties and characteristics of material products. Conventional processes for synthesizing boehmite nanostructures include sol–gel,³⁶ precipitation,³⁷ hydrothermal,^{20,30} solvothermal¹⁹ and other related routes. Among the reported synthetic routes, the solvothermal technique has been broadly employed as an effective method due to its mild synthesis conditions and flexible changes of experimental parameters, and is an economic and versatile method for the preparation of low-dimensional nanomaterials with controllable sizes and shapes. In this method, the synthesis conditions, such as solvent, reaction temperature and time, solution pH, addition of surfactants and pH adjustment reagents, have great effects on the structure and character of boehmite.^{19,20,28,30,31,38} Undoubtedly; the research and development of producing AlOOH with various structures are beneficial for many branches of modern science and technology.

Herein, a new and facile route to the fabrication and growth of boehmite nanostructures is presented, in which the effect of pH was investigated.

EXPERIMENTAL

The utilized starting materials were Al(NO₃)₃·9H₂O, NaOH, and absolute ethanol, which were purchased from Scharlau, Spain, and used without further purification.

Typically, 5 g Al(NO₃)₃·9H₂O was dissolved in 60 mL of ethanol and stirred for 5 min at room temperature. NaOH solution (2 M) was subsequently added dropwise to the solution to give lacteous precipitates. At this point, the pH value of the reaction mixture was ≈3, 4.5, 6.5, 10 or 12.5. The mixture was then transferred into a Teflon-lined stainless steel autoclave and heated at 180 °C for 24 h (the corresponding pressure was 19.4 atm according to Antoine Equation calculation).³⁹ These samples were treated by centrifugation, rinsed with ethanol 96 % several times, and then dried overnight at 60 °C in an oven. The prepared boehmite samples were labelled N-3, N-4.5, N-6.5, N-10 and N-12.5.

FTIR spectroscopy was performed using a Rayleigh WQF-510 spectrometer in the range of 400–4000 cm⁻¹ at room temperature. Powder X-ray diffraction (XRD) analysis was performed on a Bruker B8 Advance diffractometer. The X-ray patterns were recorded in step

scanning using $\text{CuK}\alpha$ radiation ($\lambda = 1.54 \text{ \AA}$) at a scan rate of 1° min^{-1} in the 2θ range 5 to 85° . The surface morphology and particles sizes were analysed by a field emission scanning electron microscope (FESEM, Hitachi S-4160 XL30). The specific surface area of the synthesised samples was determined using a BEL SORP, Mini II-310 analyser. In this technique, the Brunauer–Emmett–Teller (BET) equation⁴⁰ was employed to calculate the specific surface area, and the mean pores size were calculated using the original Barrett, Joyner and Halenda (BJH) method.⁴¹

RESULTS AND DISCUSSION

The phase composition of the samples was examined by XRD. The XRD patterns of the samples synthesized solvothermally for 24 h at different pH levels are shown in Fig. 1. When compared to the standard pattern, the reflections of all samples were readily indexed to the orthorhombic boehmite phase γ -AlOOH (JCPDS No. 021-1307), and no other peaks belonging to impurities could be observed, indicating the high purity of the products. The results indicate that the obtained AlOOH can be indexed to an orthorhombic cell with lattice parameters of $a = 3.7 \text{ \AA}$, $b = 12.227 \text{ \AA}$, and $c = 2.867 \text{ \AA}$. It could be seen that there was no

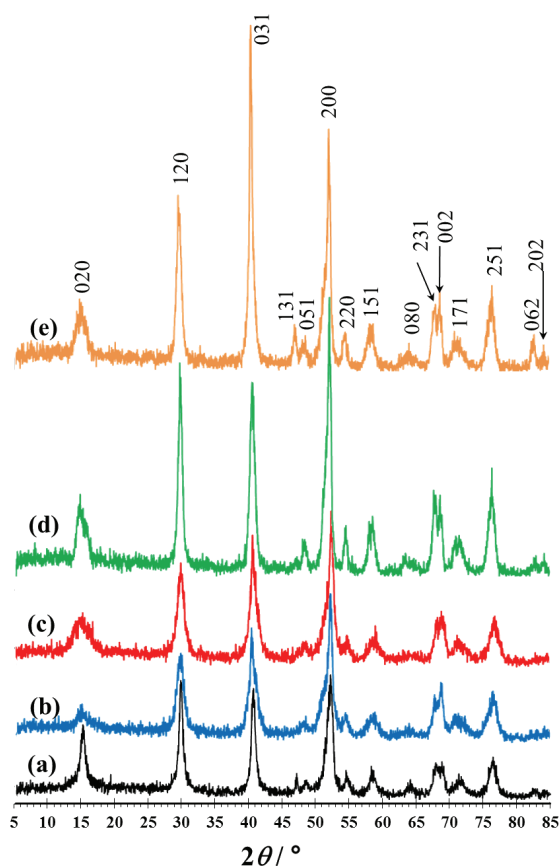


Fig 1. XRD patterns of the as-synthesized: a) N-3, b) N-4.5, c) N-6.5, d) N-10 and e) N-12.5 sample.

linear increase in any specific diffraction peak with increasing pH of the solution. On the other hand, the intensities for most of the diffraction peaks gradually increased with the increasing of pH of solution. Moreover, the peak intensity of (031) increased with increasing the solution pH from 4.5 to 12.5, indicating improved crystallization and particle growth. This phenomenon was demonstrated in some research papers, which showed that with increasing particle size, the peak intensities for the materials increased.^{42,43} Additionally, it was noted that the diffraction peaks in the XRD patterns of the samples were of high intensity and narrow, which indicates the good crystallinity of the samples, especially for the boehmite synthesized in the basic pH solution.

The crystallite sizes were calculated using the Scherrer equation, $d = (k\lambda) / (L\cos\theta)$, where k is a dimensionless shape factor, λ is the wavelength of the X-rays, L is the full width of diffraction peak at half maximum intensity (FWHM), and θ is the Bragg angle. The calculated crystallite sizes of N-3, N-4.5, N-6.5, N-10 and N-12.5 samples were 12.5, 9.3, 9.4, 13.2 and 20.5 nm, respectively (crystallite sizes calculated by using average of three highest peaks: (120), (031) and (200)). Comparison of XRD patterns of the prepared samples showed that the pH of solution influenced the size of the crystallite phase of samples, and the extent and intensity of crystallinity of samples increased with increasing the pH solution from 4.5 to 12.5.

The effects of the solution pH on the FTIR spectra of the AlOOH architectures are shown in Fig. 2. Generally, the FTIR spectra were similar for all samples, regardless of the difference in the peak intensities. There are two regions ($400\text{--}2500\text{ cm}^{-1}$ and $2500\text{--}4000\text{ cm}^{-1}$) for the samples. In the region of

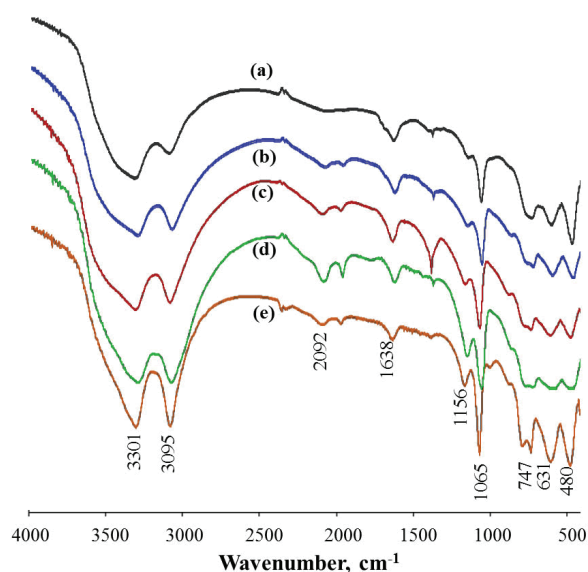


Fig 2. FTIR spectra of the synthesized samples: a) N-3, b) N-4.5, c) N-6.5, d) N-10 and e) N-12.5.

400–2500 cm^{-1} , well-resolved sharper bands were observed. As could be seen in Fig. 2, five strong bands were observed for the boehmite samples at 480, 631, 747, 1065 and 1156 cm^{-1} .⁴⁴ The sharp band at 480 cm^{-1} is assigned to the angle deformation of O=A–(OH), which results in the peaks at 631 and 747 cm^{-1} , attributed to the (AlO)–O–H angle bending.^{20,38} The intensity of these bands was stronger for the sample synthesised at pH of 12.5. The sharp peak at 1065 cm^{-1} and small shoulder at 1156 cm^{-1} are assigned to the (OH)–Al=O asymmetric stretching vibrations and O–H bending, respectively. The acute peak at 1385 cm^{-1} corresponds to the nitrate anion, which was not thoroughly removed by washing. As a comparison, the intensity of this band is stronger for the synthesized sample with pH 6.5 as it had not been washed well. The band at 1640 cm^{-1} could be assigned to bending vibrations⁴⁵ of the OH group from adsorbed water. In the region 2500–4000 cm^{-1} , the samples showed two broad and resolved bands at 3095 and 3301 cm^{-1} , which could be assigned to the $\nu_{\text{as}}(\text{Al})\text{O–H}$ and $\nu_{\text{s}}(\text{Al})\text{O–H}$ stretching vibrations. These two bands became sharper with increasing of pH, which indicates the high crystallinity⁴⁶ of samples prepared in the basic pH value.

It was very interesting to find that the pH of solution had a considerable effect on the morphologies of the as-prepared boehmite. FESEM analysis was conducted to represent clearly the structural characteristics of the samples. Representative FESEM images of samples are shown in Fig. 3. Lower and higher magnification analyses were performed on all samples. According to Fig. 3a, the N-3 sample had a different shape compared with other prepared samples, and consisted of more nano-layers with a mean width size of around 40 nm. However, on increasing the pH of the solution to 4.5, the final product was mainly composed of many uniform particles with an average size of 35 nm (Fig. 3b). When the pH was increased to 6.5, the particle size became larger than the particle size in N-4.5. When the pH of the solution was increased from 4.5 to 12.5, the obtained micrograph images, regarding the increasing crystallinity and particle size, were in agreement with and confirmed the results of the FTIR spectra and the obtained XRD patterns.

In general, the average size of the particles in the synthesized samples regularly increased from almost 35 to 57 to 155 to 542 nm on increasing of pH from 4.5 to 6.5 to 10 to 12.5, respectively. The histograms of the particle size distribution for the samples are shown in Fig. 4. According to these results, the pH of solution had strong effects on the particle size and formation of boehmite by the solvothermal method.

The porous structure and texture of the samples were investigated by N_2 adsorption/desorption analysis. The results of the textural properties, and porosity structures and positions of the synthesized AlOOH nanostructures are listed in Table I. These results imply that the pH is quite important in the preparation of AlOOH by the solvothermal method.

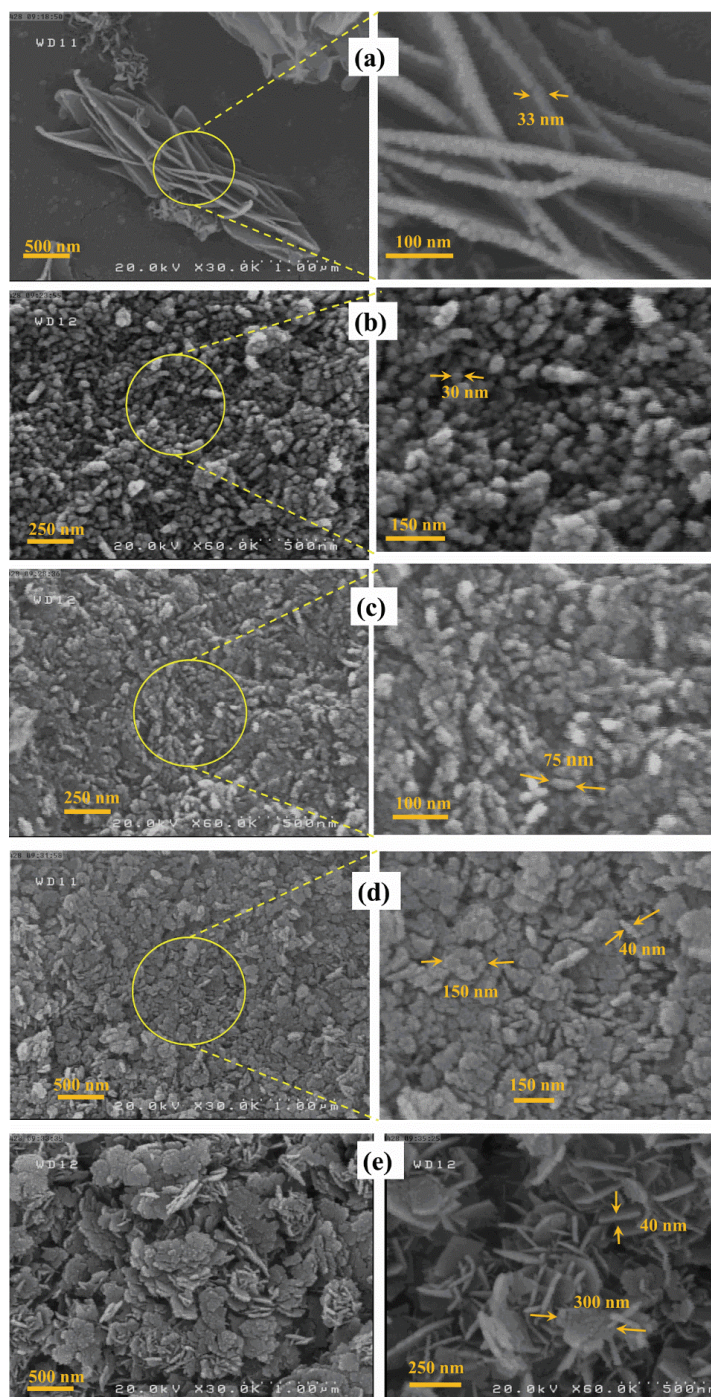


Fig. 3. FESEM images of: a) N-3, b) N-4.5, c) N-6.5, d) N-10 and e) N-12.5.

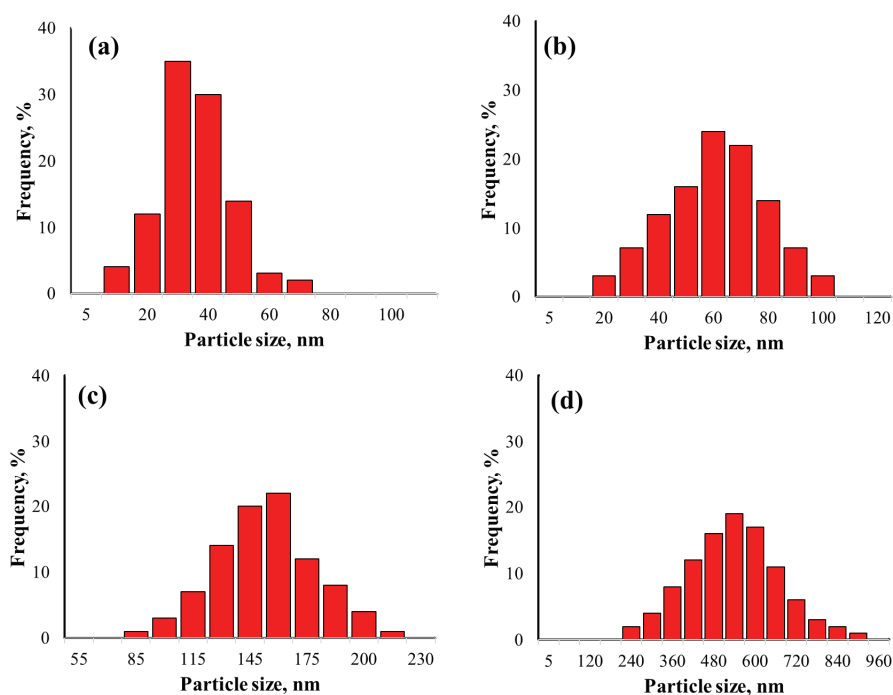


Fig. 4. Histograms showing the particle size distribution in: a) N-4.5, b) N-6.5, c) N-10 and d) N-12.5.

TABLE I. Textural properties of the synthesized boehmite samples

Sample	Microporosity, %		Mesoporosity, %				
	≤ 2 nm	2–5 nm	5–10 nm	10–15 nm	15–25 nm	25–40 nm	40–50 nm
N-3	10.5	15.3	24.6	26.2	20.7	1.6	0.5
N-4.5	5.0	21.7	34.6	37.0	1.4	0.2	0.0
N-6.5	6.7	33.2	59.6	0.20	0.1	0.0	0.0
N-10	6.0	19.8	40.0	30.9	2.8	0.3	0.1
N-12.5	6.3	27.3	33.3	15.7	10.7	5.3	1.1

The nitrogen adsorption–desorption isotherms and the corresponding pore-size distribution curves (inset) for all the prepared samples are shown in Fig. 5. All the samples exhibit type IV with a type H2 hysteresis loop, except for N-12.5 that shows type H1.⁴⁷ These adsorption characteristics are usually attributed to adsorption in mesoporous materials, which were classified by IUPAC.⁴⁷ A comparison of all samples shows an increase in the amount of adsorbed N_2 at high relative pressures ($p/p_0 = 0.6–1.0$), especially for N-12.5, suggesting larger pore volumes for this sample. The pore size distributions calculated for all the samples are shown in the inset of Fig. 5, indicating that they are mainly in the range of 2–60 nm, which further confirms the presence of micro- and meso-pores.

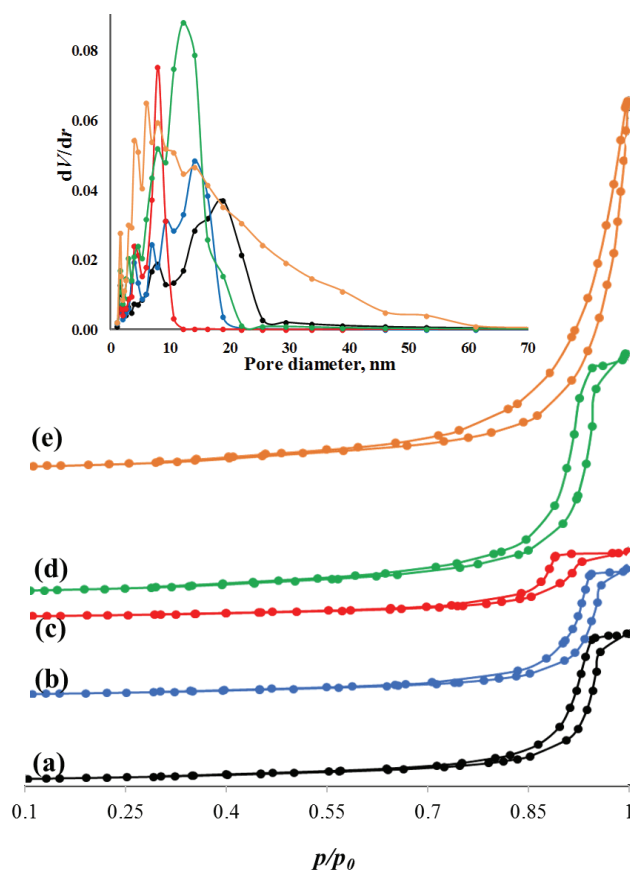


Fig. 5. Nitrogen adsorption–desorption isotherms and the corresponding pore size distribution curves (inset) for samples: a) N-3, b) N-4.5, c) N-6.5, d) N-10 and e) N-12.5.

The parameters for the pore structure for all samples including the total surface area from BET and t -plots, total pore volume from BET and BJH methods, microporosity, mesoporosity, and the average pore diameter are listed in Table II.

TABLE II. Porosity structures and positions of synthesized boehmite samples

Sample name	$S_{\text{total}}^{\text{a}}$ $\text{m}^2 \text{g}^{-1}$	$S_{\text{total}}^{\text{b}}$ $\text{m}^2 \text{g}^{-1}$	V_{p}^{c} $\text{cm}^3 \text{g}^{-1}$	V_{p}^{d} $\text{cm}^3 \text{g}^{-1}$	$V_{\text{mic}}^{\text{e}}$ $\text{cm}^3 \text{g}^{-1}$	$V_{\text{mes}}^{\text{f}}$ $\text{cm}^3 \text{g}^{-1}$	$V_{\text{mac}}^{\text{g}}$ $\text{cm}^3 \text{g}^{-1}$	D_{p}^{h} nm
N-3	65.4	83.7	0.50	0.51	0.053	0.445	0.001	15.5
N-4.5	54.6	71.3	0.42	0.43	0.021	0.399	0.000	13.1
N-6.5	46.9	62.8	0.24	0.24	0.016	0.224	0.000	7.2
N-10	99.4	136.1	0.80	0.81	0.048	0.751	0.000	11.4
N-12.5	131.0	175.4	1.24	1.23	0.078	1.159	0.003	19.2

^a Total surface area from the BET method; ^b total surface area from t -plots; ^c total pore volume from the BET method; ^d total pore volume from the BJH method; ^e microporosity; ^f mesoporosity; ^g macroporosity; ^h average pore diameter

The sample obtained at neutral pH (6.5) had the lowest surface area, pore volume, and average pore diameter, and all these characteristics increased with increasing of pH. The AlOOH synthesised at pH 12.5 showed a significant broadening of the pore size distribution and an increase in the pore size. Moreover, the N-12.5 sample exhibited a high specific surface area of $131 \text{ m}^2 \text{ g}^{-1}$ and a large pore volume of $1.24 \text{ cm}^3 \text{ g}^{-1}$. In general, larger specific surface area and pore volume are favourable for many applications, such as catalysis.^{48–50}

CONCLUSIONS

A new and facile solvothermal method was successfully utilized to produce different boehmite nanostructures with crystallite sizes of 9.3–20.5 nm, surface areas of 46–131 $\text{m}^2 \text{ g}^{-1}$, and pore volumes of 0.24–1.24 $\text{cm}^3 \text{ g}^{-1}$. The most significant aspect of the present study was that AlOOH powders could be prepared at different pH levels with controlled sizes. The results showed that AlOOH synthesized at pH 3 was a nanostructure with several nano-sized layers. Nevertheless, with increasing pH from 4.5 to 12.5, the size of particles grew from 35 to 542 nm. The sample synthesized at pH 12.5 showed a high surface area and large pore volume. It is believed that such ordered boehmite particles could have a wide range of potential applications, such as catalysis and adsorption.

Acknowledgement. The authors gratefully acknowledge the Islamic Azad University, Kermanshah Branch for their support.

ИЗВОД

НОВИ ПРИСТУП СИНТЕЗИ И РАСТ НАНОКРИСТАЛНОГ AlOOH СА ВЕЛИКОМ ЗАПРЕМИНОМ ПОРА

FARHAD SALIMI¹, MOZAFFAR ABDOLLAHIFAR^{1,2}, POURIA JAFARI¹ и MASOUD HIDARYAN¹

¹Department of Chemical Engineering, College of Science, Kermanshah Branch, Islamic Azad University, Kermanshah 67131, Iran и ²Department of Chemical Engineering, National Taiwan University, Taipei, 106, Taiwan

У овом раду је успешно синтетизован наноструктурни AlOOH солвотермалном методом на 180 °C. Детаљно је испитиван утицај рН раствора (3, 4,5, 6,5, 10 и 12,5) на својства синтетизованих узорака, при чему је етанол коришћен као растварач, а NaOH за подешавање рН раствора. За карактеризацију узорака коришћени су инфрацрвена спектроскопија са Фуријеовом трансформацијом (FTIR), рендгенска дифракциона анализа (XRD) и скенирајућа електронска микроскопија (FESEM). Вредности специфичне површине, као и расподела величина пора и структура пора добијених узорака, одређене су адсорпцијом/десорпцијом азота и анализирани у зависности од рН вредностима раствора. FESEM микрографије су показале да су добијени наноструктурни производи и да AlOOH наночестице расту са повишењем рН од 4,5 до 12,5. Структурна карактеризација је показала да су добијени узорци AlOOH добро дефинисане кристалне структуре, са кристалима димензија 9,3–20,5 nm. Бемит добијен при почетној рН 12,5 има велику специфичну површину од $131 \text{ m}^2 \text{ g}^{-1}$ и велику запремину пора од $1,24 \text{ cm}^3 \text{ g}^{-1}$.

(Примљено 13. јула, ревидирано 9. новембра, прихваћено 14. новембра 2016)

REFERENCES

1. M. Abdollahifar, M. Haghghi and A. A. Babaluo, *J. Ind. Eng. Chem.* **20** (2014) 1845
2. J. Baneshi, M. Haghghi, N. Jodeiri, M. Abdollahifar, H. Ajamein, *Energy Convers. Manage.* **87** (2014) 928
3. H. Ajamein, M. Haghghi, R. Shokrani, M. Abdollahifar, *J. Mol. Catal., A: Chem.* **421** (2016) 222
4. S. Khajeh Talkhonch, M. Haghghi, H. Ajamein, S. Minaei, M. Abdollahifar, *RSC Adv.* **6** (2014) 57199
5. S. Minaei, M. Haghghi, N. Jodeiri, M. Abdollahifar, H. Ajamein, *J. Appl. Res. Chem.* **8** (2014) 33
6. R. Shokrani, M. Haghghi, N. Jodeiri, H. Ajamein, M. Abdollahifar, *Inter. J. Hydrogen Energy* **39** (2014) 13141
7. S. R. Yahyavi, M. Haghghi, S. Shafiei, M. Abdollahifar, F. Rahmani, *Energy Convers. Manage.* **97** (2015) 273
8. M. Abdollahifar, M. Haghghi, A. A. Babaluo, S. Khajeh Talkhonch, *Ultrason. Sonochem.* **31** (2016) 173
9. S. Minaei, M. Haghghi, M. Abdollahifar, H. Ajamein, *Fuel Combust. J.* **8** (2015) 1
10. B. Y. Yeom, E. Shim, B. Pourdeyhimi, *Macromol. Res.* **18** (2010) 884
11. P. S. Jayan, N. Ananthaseshan, B. Subramaniam, M. V. Murugappan, US5782940A, 1998
12. A. Leenaars, K. Keizer, A. Burggraaf, *J. Mater. Sci.* **19** (1984) 1077
13. S. Furuta, H. Katsuki, H. Takagi, *J. Mater. Sci. Lett.* **13** (1994) 1077
14. W. Cai, J. Yu, B. Cheng, B.-L. Su, M. Jaroniec, *J. Phys. Chem., C* **113** (2009) 14739
15. B. Kindl, D. J. Carlsson, Y. Deslandes, J. M. A. Hoddenbagh, *Ceram. Int.* **17** (1991) 347.
16. C. S. Kumar, U. Hareesh, A. Damodaran, K. Warriar, *J. Eur. Ceram. Soc.* **17** (1997) 1167
17. A. Alemi, Z. Hosseinpour, M. Dolatyari, A. Bakhtiari, *Phys. Status Solidi B* **249** (2012) 1264
18. W. Guo, H. Kang, Y. Chen, B. Guo, L. Zhang, *ACS Appl. Mater. Interface*, **4** (2012) 4006
19. M. Abdollahifar, *J. Chem. Res.* **38** (2014) 154
20. M. Abdollahifar, R. M. Zamani, E. Beiygie, H. Nekouei, *J. Serb. Chem. Soc.* **79** (2014) 1007
21. J. Buitenhuis, L. N. Donselaar, P. A. Buining, A. Stroobants, H. N. Lekkerkerker, *J. Colloid Interface Sci.* **175** (1995) 46
22. D. Kuang, Y. Fang, H. Liu, C. Frommen, D. Fenske, *J. Mater. Chem.* **13** (2003) 660
23. Y. Li, J. Liu, Z. Jia, *Mater. Lett.* **60** (2006) 3586
24. Y. Zuo, Y. Zhao, X. Li, N. Li, X. Bai, S. Qiu, W. Yu, *Mater. Lett.* **60** (2006) 2937
25. Y. Zhu, H. Hou, G. Tang, Q. Hu, *Eur. J. Inorg. Chem.* **2010** (2010) 872
26. Y.-X. Zhang, Y. Jia, Z. Jin, X.-Y. Yu, W.-H. Xu, T. Luo, B.-J. Zhu, J.-H. Liu, X.-J. Huang, *CrystEngComm.* **14** (2012) 3005
27. L. Zhang, Y. J. Zhu, *J. Phys. Chem. C.* **112** (2008) 16764
28. M. Abdollahifar, *J. Appl. Chem.* **8** (2013) 69
29. M. Abdollahifar, A. R. Karami, N. Haghazari, C. Karami, *Ceram. Silikáty* **59** (2015) 305
30. E. Ameri, M. Abdollahifar, M. R. Zamani, H. Nekouei, *Ceram. Silikáty* **60** (2016) 162
31. F. Salimi, M. Abdollahifar, A. R. Karami, *Ceram. Silikáty* **60** (2016) 273
32. Z. Holkova, L. Pach, J. Majling, J. Kakos, M. Kadlecikova, *Ceram. Silikáty* **47** (2003) 149
33. H. Liang, L. Liu, Z. Yang, Y. Yang, *Cryst. Res. Technol.* **45** (2010) 195
34. V. Vatanpour, S. S. Madaeni, L. Rajabi, S. Zinadini, A. A. Derakhshan, *J. Membr. Sci.* **401–402** (2012) 132

35. L. Yuanyuan, J. Liu, Z. Jia, *Mater. Lett.* **60** (2006) 3586
36. Z. Q. Yu, C. X. Wang, X. T. Gu, C. Li, *J. Lumin.* **106** (2004) 153
37. D. Panias, A. Krestou, *Powder Technol.* **175** (2007) 163
38. N. Haghazari, M. Abdollahifar, F. Jahani, *J. Mex. Chem. Soc.* **58** (2014) 95
39. DDBST, <http://ddbonline.ddbst.com/AntoineCalculation/AntoineCalculationCGI.exe>, (09/02/2016)
40. S. Brunauer, P.H. Emmett, E. Teller, *J. Am. Chem. Soc.* **60** (1938) 309
41. E.P. Barrett, L.G. Joyner, P.P. Halenda, *J. Am. Chem. Soc.* **73** (1951) 373
42. M. K. Min, J. Cho, K. Cho, H. Kim, *Electrochim. Acta* **45** (2000) 4211
43. T. Drezen, N. H. Kwon, P. Bowen, I. Teerlinck, M. Isono, I. Exnar, *J. Power Sources* **174** (2007) 949
44. W. Cai, J. Yu, S. Gu, M. Jaroniec, *Cryst. Growth Des.* **10** (2010) 3977
45. H. S. Potdar, K. W. Jun, J. W. Bae, S. M. Kim, Y. J. Lee, *Appl. Catal. A* **321** (2007) 109
46. S. Musića, D. Dragčevića, S. Popović, *Mater. Lett.* **40** (1999) 269
47. K. S. W. Sing, D. H. Everett, R. A. W. Haul, L. Moscou, R. A. Pierotti, J. Rouquerol, T. Siemieniowska, *Pure Appl. Chem.* **57** (1985) 603
48. M. Sharifi, M. Haghghi, M. Abdollahifar, *Mater. Res. Bull.* **60** (2014) 328
49. M. Abdollahifar, M. Haghghi, M. Sharifi, *Energ. Convers. Manage.* **103** (2015) 1101
50. M. Sharifi, M. Haghghi, M. Abdollahifar, *J. Nat. Gas Sci. Eng.* **23** (2015) 547.